AMERICAN SOCIETY FOR MICROBIOLOGY | Molecular and Cellular Biology®

RESEARCH ARTICLE

A Homeostatic Shift Facilitates Endoplasmic Reticulum Proteostasis through Transcriptional Integration of Proteostatic Stress Response Pathways

Liam Baird,[a] Tadayuki Tsujita,[b] Eri H. Kobayashi,[a] Ryo Funayama,[c] Takeshi Nagashima,[c] Keiko Nakayama,[c] Masayuki Yamamoto[a,d]

Department of Medical Biochemistry, Tohoku University Graduate School of Medicine, Sendai, Japan[a]; Laboratory of Biochemistry, Department of Applied Biochemistry and Food Science, Faculty of Agriculture, Saga University, Saga, Japan[b]; Division of Cell Proliferation, Tohoku University Graduate School of Medicine, Sendai, Japan[c]; Tohoku Medical Megabank Organization, Sendai, Japan[d]

ABSTRACT Eukaryotic cells maintain protein homeostasis through the activity of multiple basal and inducible systems, which function in concert to allow cells to adapt to a wide range of environmental conditions. Although the transcriptional programs regulating individual pathways have been studied in detail, it is not known how the different pathways are transcriptionally integrated such that a deficiency in one pathway can be compensated by a change in an auxiliary response. One such pathway that plays an essential role in many proteostasis responses is the ubiquitin-proteasome system, which functions to degrade damaged, unfolded, or short half-life proteins. Transcriptional regulation of the proteasome is mediated by the transcription factor Nrf1. Using a conditional knockout mouse model, we found that Nrf1 regulates protein homeostasis in the endoplasmic reticulum (ER) through transcriptional regulation of the ER stress sensor ATF6. In Nrf1 conditional-knockout mice, a reduction in proteasome activity is accompanied by an ATF6-dependent downregulation of the endoplasmic reticulum-associated degradation machinery, which reduces the substrate burden on the proteasome. This indicates that Nrf1 regulates a homeostatic shift through which proteostasis in the endoplasmic reticulum and cytoplasm are coregulated based on a cell's ability to degrade proteins.

KEYWORDS ER stress, ERAD, Nrf1, proteasome, proteostasis, UPR

Received 1 August 2016 **Returned for modification** 27 August 2016 **Accepted** 23 November 2016

Accepted manuscript posted online 5 December 2016

Citation Baird L, Tsujita T, Kobayashi EH, Funayama R, Nagashima T, Nakayama K, Yamamoto M. 2017. A homeostatic shift facilitates endoplasmic reticulum proteostasis through transcriptional integration of proteostatic stress response pathways. Mol Cell Biol 37:e00439-16. https://doi.org/10.1128/MCB.00439-16.

Address correspondence to Liam Baird, liambaird@med.tohoku.ac.jp, or Masayuki Yamamoto, masiyamamoto@med.tohoku.ac.jp.

The maintenance of protein homeostasis is an essential characteristic of life. Orchestrated by conserved basal and inducible systems, the activity of a cell's proteome is optimized to facilitate maximal biological activity across a range of environmental conditions. Reflecting the fundamental importance of these processes, such "proteostasis" networks are found in all three domains of life (1).

In eukaryotes, the concerted action of chaperones, folding factors, and degradation systems allows cells to maintain proteostasis and counteract protein misfolding and aggregation in the face of cellular stress. As such, the failure of these proteostasis mechanisms is a hallmark of aging and underlies many human diseases, including neurodegenerative diseases and cancer (2–5).

The regulation of proteostasis is of particular importance in the endoplasmic reticulum (ER), as approximately one-third of eukaryotic proteins enter the ER to undergo conformational folding and assembly prior to entry into the secretory pathway (6, 7). Changes in ER homeostasis, caused by a wide range of environmental perturbations, including energy deprivation, redox imbalance, and inflammation, lead to the accumulation of unfolded proteins in the ER lumen, resulting in ER stress and the

activation of the unfolded protein response (UPR) (5, 8). The UPR is regulated by the ER-resident sensor proteins IRE1, PERK, and ATF6, which function in concert to restore ER homeostasis by expanding the ER, inhibiting protein translation, increasing protein-folding capacity or, under conditions of sustained stress, promoting apoptosis (9–13).

ER-resident chaperones both assist protein folding and function in the ER quality control pathway. Through this process, chaperones evaluate the conformation of their substrates, with correctly folded proteins being targeted to the Golgi or cell membrane, and non-natively folded proteins being subject to either additional refolding cycles or degradation though the ER-associated degradation (ERAD) pathway (6, 7). ERAD involves the retrotranslocation and ubiquitination of unfolded ER proteins prior to their degradation by the cytosolic ubiquitin-proteasome system (UPS). The UPS plays a central role in eukaryotic proteostasis by regulating the cytosolic degradation of proteins. UPS substrates are targeted for degradation by the proteasome through a tightly regulated ubiquitin ligase-mediated polyubiquitination-dependent mechanism. Since the proteasome is also the site of ERAD-dependent protein degradation, it plays a critical role in both cytoplasmic and ER homeostasis (6, 14–16).

The cap'n'collar (CNC)/bZIP transcription factor Nrf1 (*NFE2L1*) regulates the transcription of the proteasome subunit genes and, as such, plays a key role in modulating the activity of the UPS (17, 18). Nrf1 knockout mice die during embryogenesis due to a defect in liver erythropoiesis, whereas liver- and brain-specific conditional knockout mice revealed that Nrf1 plays a key role in regulating cell survival and energy metabolism (19–24). Subcellular localization experiments suggest that in nonstressed conditions, Nrf1 is targeted to the ER membrane; however, the signals that activate Nrf1, and the role that it plays in regulating ER homeostasis, have not been delineated (25, 26).

Although the details of individual proteostasis pathway are well understood, it is not known how these pathways can compensate for one another when the activity of a single pathway is reduced. Understanding the interactions between these pathways is particularly important given the fact that disruption of proteostasis networks is a frequent event in human disease (2, 4, 5).

To study how cells adapt to a reduction in proteasome activity, we utilized an Nrf1 conditional knockout (CKO) mouse model in which the expression of the proteasome subunit genes is significantly downregulated. We found that the ER stress sensor ATF6 is downregulated in Nrf1 CKO mice, while chromatin immunoprecipitation followed by massively parallel sequencing (ChIP-Seq) revealed that Nrf1 directly regulates the expression of ATF6. In keeping with the role of ATF6 in regulating ERAD, we found that many ERAD components are downregulated in Nrf1 CKO mice, which would function to reduce the flow of protein substrates to the proteasome. Together, these data suggest that the proteasome, UPR, and ERAD transcriptional programs are functionally integrated in order to allow cells to adapt to a change in activity of the individual components and that the loss of Nrf1 leads to a homeostatic shift through which ERAD is downregulated.

RESULTS

Expression of the ER stress sensor gene *Atf6* is downregulated in Nrf1 CKO mice. Due to its fundamental role in the regulation of proteasome subunit gene expression, coupled with the fact that, as the final site of ubiquitinated protein degradation, the proteasome plays a central role in endoplasmic reticulum-associated degradation (ERAD), we hypothesized that Nrf1 may regulate ER homeostasis and thus be transcriptionally integrated into the unfolded protein response (UPR) pathway. To test this hypothesis in an *in vivo* mammalian model, we utilized a recently generated Nrf1 conditional knockout mouse line, in which the *Nrf1* gene is deleted in the liver during adulthood. In this model, expression of the Cre recombinase is dependent on the activity of the *CYP1A1* promoter. Thus, adult-specific *CYP1A1* expression is induced by the injection of 3-MC, resulting in the excision of *Nrf1* in the liver (23).

In keeping with previous reports, the liver-specific conditional knockout of *Nrf1* resulted in the significant downregulation of proteasome subunit expression (17, 18).

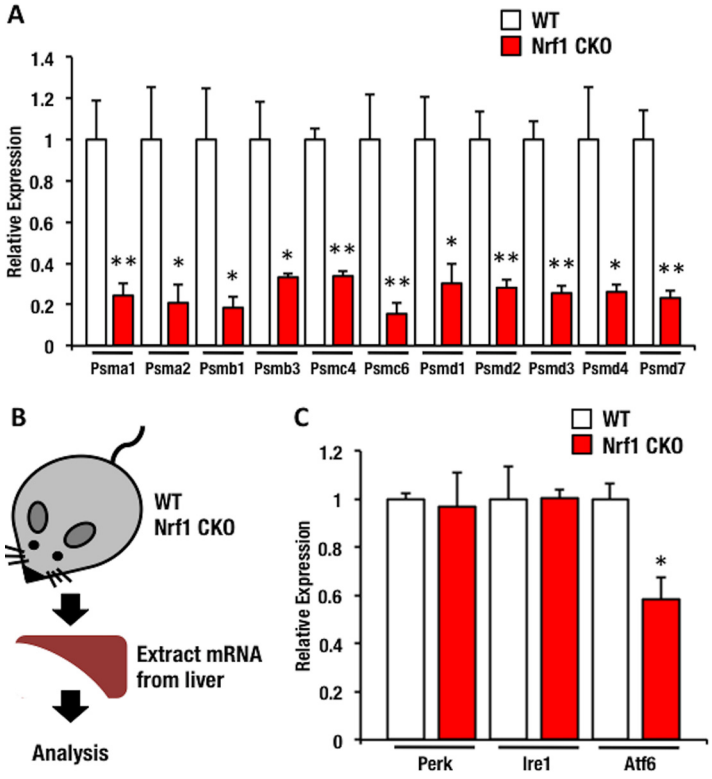

FIG 1 The ER stress sensor gene *Atf6* is significantly downregulated in Nrf1 CKO mice. (A) RT-qPCR analysis of wild-type and Nrf1 CKO liver tissue shows that a broad range of proteasome subunits are significantly downregulated in Nrf1 CKO mice. (B) Schematic representation of the experimental approach. mRNA was extracted from the livers and used for RT-qPCR analysis of gene expression. (C) RT-qPCR analysis of the expression of the ER stress sensor genes *Perk*, *Ire-1*, and *Atf6* clearly shows that while the expression of *Perk* and *Ire-1* are unaltered in Nrf1 CKO liver, *Atf6* is significantly downregulated in the absence of Nrf1. In both panels A and C, gene expression in Nrf1 CKO liver tissue is shown relative to the wild type, with wild-type expression fixed at 1. Error bars display the SEM ($n = 4$; *, $P < 0.05$; **, $P < 0.01$).

Thus, quantitative reverse transcription-PCR (RT-qPCR) revealed that representative genes from all four proteasome subunit families, *Psma*, *Psmb*, *Psmc*, and *Psmd*, were significantly downregulated in the absence of Nrf1 (Fig. 1A). In addition to degrading cytoplasmic proteins, the proteasome also degrades ER-resident proteins that have been retrotranslocated to the cytoplasm through the process of ERAD (7). Since ER homeostasis is regulated by the UPR, we hypothesized that a change in proteasome activity would impact ER proteostasis, and thus a reduction in Nrf1 activity may be accompanied by a concomitant change in the UPR.

The UPR is regulated by the ER-resident sensory proteins PERK, IRE1, and ATF6. Therefore, we wanted to determine whether the expression of these sensor proteins is differentially modulated in *Nrf1* CKO mice under basal conditions (Fig. 1B). Although *Perk* and *Ire1* showed no difference in expression between wild-type (WT) and Nrf1 CKO mice, *Atf6* mRNA was significantly downregulated (Fig. 1C). This suggests that Nrf1 specifically regulates *Atf6* expression and thus is transcriptionally integrated into the UPR and ER homeostasis pathways.

Nrf1 ChIP-Seq for the assessment of ER homeostasis regulation. Since target gene output of Nrf1 signaling is poorly understood, we carried out chromatin immunoprecipitation followed by massively parallel sequencing (ChIP-Seq) in order to determine exactly how Nrf1 regulates ER proteostasis.

Since, to our best knowledge, ChIP-Seq analysis has not previously been carried out on Nrf1, we selected mouse embryonic fibroblasts (MEFs) as our model system because they accumulate Nrf1 in response to proteasome inhibitors and would allow us to use

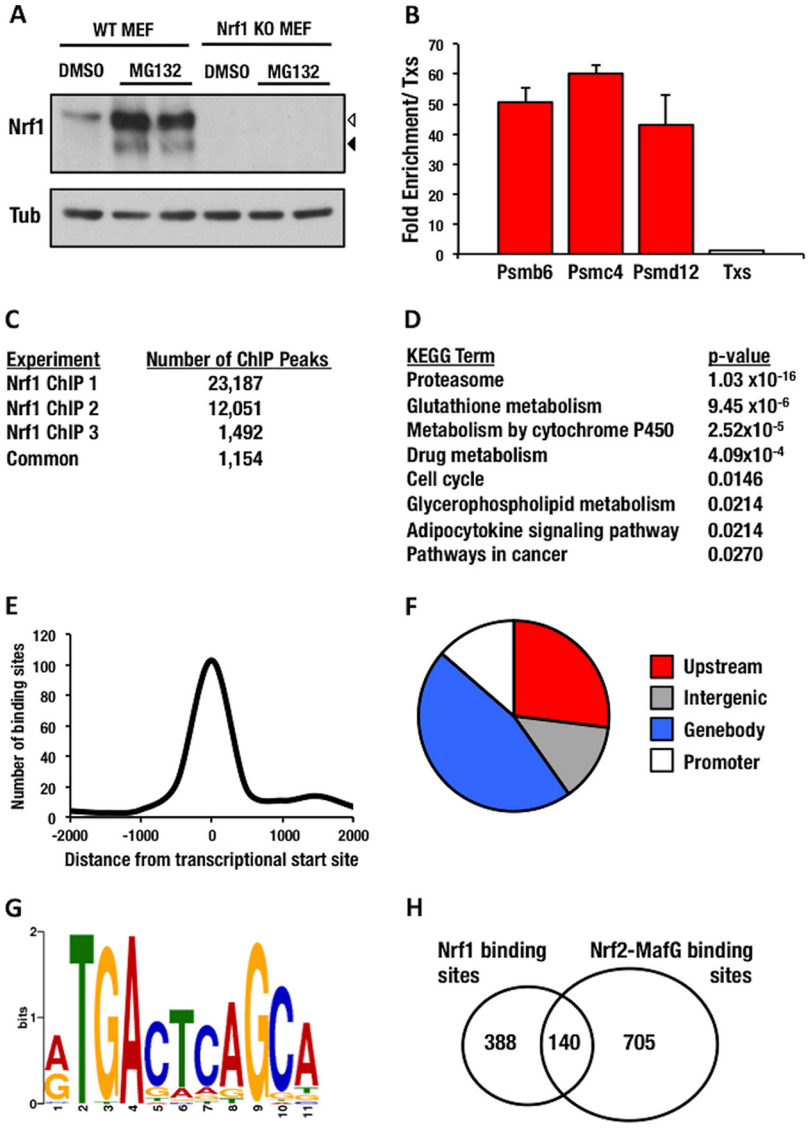

FIG 2 ChIP-Seq analysis of Nrf1. (A) Wild-type MEFs were used for the ChIP-Seq experiments. In response to the proteasome inhibitor MG132, the Nrf1 protein significantly accumulates within cells. Two isoforms of Nrf1 are present in MEFs: a high-molecular-weight form (open triangle) and a cleaved low-molecular-weight nuclear form (closed triangle). (B) Manual ChIP-qPCR of the Nrf1 target genes *Psmb6*, *Psmc4*, and *Psmd12* showed significant enrichment during pulldown with the TFC11 antibody compared to the control locus Txs. Error bars display the SEM ($n = 3$). (C) Summary of the three Nrf1 ChIP-Seq data sets. Library 3 contains the most highly enriched peaks from libraries 1 and 2, suggesting that it was created using more stringent conditions. (D) KEGG pathway analysis of the genes associated with the Nrf1 binding peaks identified from the ChIP-Seq data. (E) The relative distance of the identified Nrf1 binding sites relative to the transcriptional start site (TSS) shows clear clustering around the TSS. (F) Genomic distribution of the Nrf1 binding peaks identified by ChIP-Seq. (G) The consensus Nrf1 binding site identified using MEME-ChIP. (H) Comparison of binding site locations between Nrf1 and a previously published Nrf2-sMaf ChIP-Seq analysis.

Nrf1 knockout (KO) MEFs as a negative control during the ChIP optimization. In the basal state, Nrf1 is present at a low level in MEF cells; however, upon MG132-mediated proteasome inhibition, Nrf1 is stabilized and accumulates within the cells. It has been reported that cleavage of Nrf1 is required for nuclear localization, and thus proteasome inhibition results in the appearance of a smaller, faster-migrating form of Nrf1, which can translocate to the nucleus to regulate target gene expression (17, 27) (Fig. 2A, closed triangle).

Using the previously identified Nrf1 proteasome target genes *Psmb6*, *Psmc4*, and *Psmd12* as positive controls, we optimized the ChIP protocol to achieve significant

TABLE 1 Location of Nrf1 binding sites in the promoters of proteasome subunit genes[a]

Family and gene	Nrf1 ChIP-Seq peak distance from TSS (bp)	Family and gene	Nrf1 ChIP-Seq peak distance from TSS (bp)
Psma		Psmd	
Psma1	0	*Psmd1*	0
Psma2	0	*Psmd2*	32
Psma3	0	*Psmd3*	0
Psma4	0	*Psmd4*	0
Psma5	254	*Psmd5*	990
Psma6	18	*Psmd6*	25
Psma7	459	*Psmd7*	0
		Psmd8	0
Psmb		*Psmd9*	288
Psmb1	0	*Psmd10*	0
Psmb2	0	*Psmd11*	118
Psmb3	0	*Psmd12*	0
Psmb4	0	*Psmd13*	0
Psmb5	0	*Psmd14*	26
Psmb6	0		
Psmb7	2	Psme	
		Psme1	6,312
Psmc		*Psme3*	137
Psmc1	1,839	*Psme4*	1,378
Psmc2	1,358		
Psmc3	25		
Psmc4	0		
Psmc5	0		
Psmc6	73		

[a]The distances shown are relative to the transcriptional start sites (TSS) defined by the RefSeq database.

enrichment for Nrf1 binding as assayed by manual ChIP-qPCR (Fig. 2B). Using this protocol, we generated three Nrf1 ChIP libraries, which were each subjected to next-generation sequencing. Each ChIP library was generated from an independent experiment, with library 3 containing the fewest binding peaks (Fig. 2C). The peaks in library 3 represented the most highly enriched peaks from libraries 1 and 2, suggesting that the conditions used during the construction of library 3 were more stringent than for libraries 1 and 2. Thus, the vast majority of the 1,492 peaks found in library 3 were also found in libraries 1 and 2, with 1,154 peaks being conserved across the libraries. Therefore, these common ChIP-Seq peaks were used for further analysis.

As expected, the ChIP-Seq analysis identified Nrf1 binding sites in the promoters for all seven of the proteasome subunit genes in the Psma family, all seven of the genes in the Psmb family, all six genes in the Psmc family and all 14 members of the Psmd family (Table 1). KEGG pathway analysis of the Nrf1 binding sites suggested that, in addition to its role in regulating the proteasome, Nrf1 also regulates other cellular processes, including glutathione metabolism and cytochrome P450-dependent metabolism (Fig. 2D).

In keeping with Nrf1's role as a transcription factor, these peaks were highly clustered around the transcriptional start sites (TSS) of genes (Fig. 2E). On a genomic scale, 14% of Nrf1 binding sites were located in the promoter region (defined as ranging from kb −2 to +0.5 relative to the TSS), 27% were located in upstream enhancer regions (defined as ranging from kb −20 to −2 relative to the TSS), 46% were located in the gene body (ranging from kb +0.5 relative to the TSS to kb +1 relative to the transcription termination site [TTS]), and 13% located in the intergenic regions (Fig. 2F).

Consistent with Nrf1 being a member of the CNC/bZIP family of transcription factors, analysis of the ChIP-Seq data set revealed the consensus Nrf1 binding site to be (A/G)TGACTCAGC (Fig. 2G), which is the same sequence that was identified for the closely related factor Nrf2 (28, 29). Despite the identical nature of the Nrf1 and Nrf2 consensus binding sites, a comparison of the location of their binding sites within the

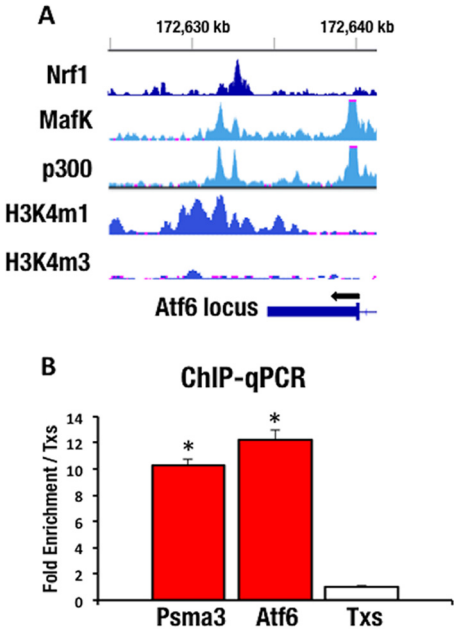

FIG 3 Nrf1 binds to an enhancer in the *Atf6* locus. (A) Nrf1 ChIP-Seq binding site in the *Atf6* locus, coupled with binding sites for MafK, p300, H3K4m1, and H3K4m3 obtained from the USC genome browser (https://genome.ucsc.edu). (B) Manual ChIP-qPCR showing enrichment of Nrf1 at the *Psma3* and *Atf6* loci relative to the negative control, *Txs*. Error bars display the SEM ($n = 3$; *, $P < 0.001$).

genome revealed limited overlap, with only 27% of genes which contained an Nrf1 binding site also containing a binding site for Nrf2 (Fig. 2H). This suggests that some other, as yet unidentified, factor(s) must play a major role in determining the binding site preference for Nrf1 and Nrf2.

Nrf1 directly regulates *Atf6* expression. Consistent with the reduced expression of *Atf6* observed in the Nrf1 CKO mouse liver, we identified an Nrf1 binding site in the *Atf6* locus. Importantly, this binding site was at the same location as has previously been identified for Nrf1's heterodimerization partner MafK and its transcriptional coactivator p300, suggesting that this site is functionally important (Fig. 3A) (30–32; http://genome.ucsc.edu). Furthermore, ChIP-Seq data for the histone modifications H3K4me1 and H3Kme3 indicated that this site functions as an active enhancer (Fig. 3A) (31, 33; http://genome.ucsc.edu). The significance of Nrf1 binding to the *Atf6* locus was confirmed by ChIP-qPCR, with 12-fold enrichment of Nrf1 at the *Atf6* site compared to the negative control locus *Txs* ($P < 0.001$) (Fig. 3B). Importantly, the enrichment of Nrf1 at the *Atf6* locus was similar to that of the positive-control locus *Psma3* (10-fold enrichment, $P < 0.001$) (Fig. 3B). Together, these data suggest that Nrf1 actively regulates *Atf6* expression by binding to an enhancer element within its locus and thus regulates ER homeostasis through the direct transcriptional regulation of the ER stress sensor gene *Atf6*.

ERAD is downregulated in Nrf1 CKO mice. Since ATF6 is involved in the transcriptional regulation of the ERAD machinery, we reasoned that Nrf1 may regulate ER proteostasis by modulating the ATF6-dependent ERAD pathway (34, 35). To confirm this hypothesis, we carried out a microarray using the livers from WT and Nrf1 CKO mice under basal conditions (Fig. 4). Analysis of this array confirmed the role of Nrf1 in the regulation of the proteasome (Fig. 4A). Significantly, both *Atf6*, and a number of ATF6 target genes, were also found to be downregulated in Nrf1 CKO mice, suggesting that Nrf1-mediated regulation of *Atf6* is functionally important and leads to a reduction in the ATF6-dependent transcription program (Fig. 4B). Interestingly, in addition to ATF6-dependent genes, a number of other ER protein processing and ERAD-associated genes were also found to be downregulated in the Nrf1 CKO mice (Fig. 4C). Together, these

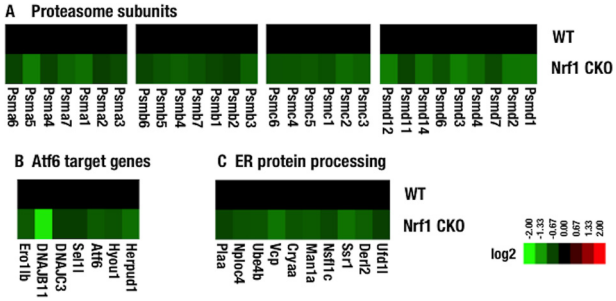

FIG 4 Microarray analysis shows a significant change in ER homeostasis gene expression in Nrf1 CKO mice. A microarray performed comparing gene expression in Nrf1 CKO liver and WT liver tissue revealed downregulation of proteasome subunit genes (A), the ATF6-dependent transcription program (B), and genes involved in protein processing in the ER (C).

data suggest that Nrf1 is an integral member of the homeostatic network that regulates the ER.

The ATF6 transcriptional program is downregulated in Nrf1 CKO mice. In order to validate the microarray results, we carried out manual qPCR for ATF6 target genes. Importantly, we found that both ATF6's chaperone target genes, including *DNAJC3* and *Hyou1*, as well as its ERAD target genes, *Herpud1* and *Sel1l*, were significantly downregulated in Nrf1 CKO mice, suggesting a comprehensive downregulation of the ATF6 transcriptional program in the absence of Nrf1 (Fig. 5A) (34–36).

The downregulation of ATF6 at the protein level was confirmed by immunoblot analysis, which clearly showed that in comparison with WT mice, ATF6 is significantly downregulated in Nrf1 CKO liver tissue (Fig. 5B). In addition, RT-qPCR confirmed that the ERAD components *Nploc4*, *Ufd1l*, and *Derl2* were also significantly downregulated in Nrf1 CKO mice, suggesting a broad modulation of the ERAD pathway, which extends beyond ATF6 regulation, in the absence of Nrf1 (Fig. 5C) (7). Together, these data

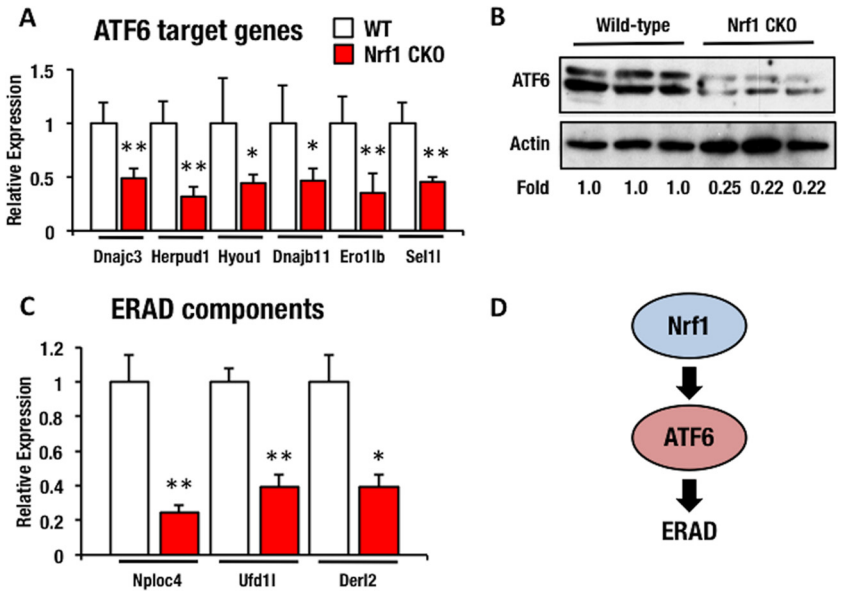

FIG 5 The ATF6 and ERAD transcriptional programs are downregulated in Nrf1 CKO mice. (A) RT-qPCR of ATF6 target genes revealed that they are significantly downregulated in Nrf1 CKO liver in comparison to wild-type tissue. (B) Immunoblot analysis of three wild-type and Nrf1 CKO mice clearly shows that, at the protein level, the cellular abundance of ATF6 is reduced in Nrf1 CKO cells. (C) RT-qPCR analysis of additional ERAD components shows that they are significantly downregulated in Nrf1 CKO liver tissue. (D) Diagram showing the proposed mechanism by which Nrf1 regulates ER homeostasis. In the absence of Nrf1, the transcription factor ATF6 is downregulated, leading to a decrease in ERAD. In both panels A and C, the error bars display the SEM ($n = 4$; *, $P < 0.05$; **, $P < 0.01$).

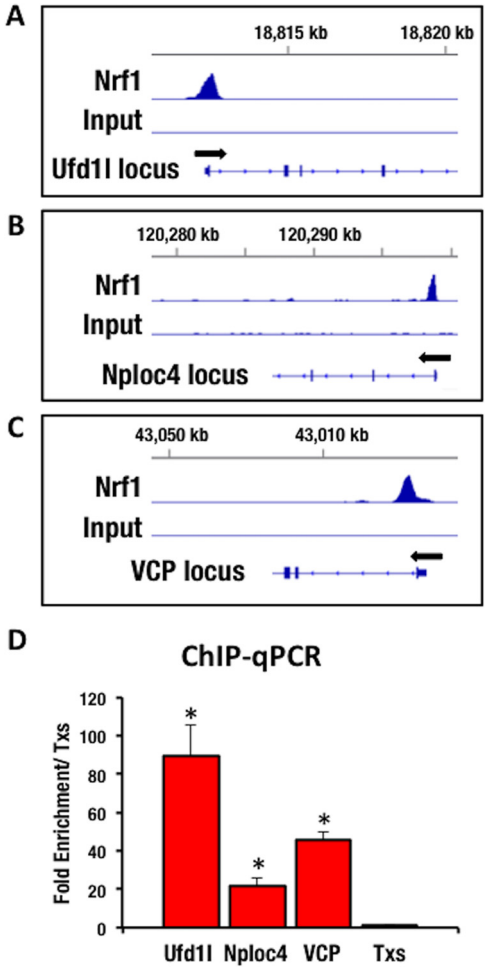

FIG 6 Nrf1 directly regulates transcription of the ERAD machinery. Nrf1 ChIP-Seq binding sites in the promoters of the *Ufd1l* (A), *Nploc4* (B), and *VCP* (C) genes are shown. (D) A manual ChIP-qPCR shows enrichment of Nrf1 at the *Ufd1l*, *Nploc4*, and *VCP* loci relative to the negative control, *Txs*. Error bars display the SEM ($n = 3$; *, $P < 0.005$).

demonstrate that in Nrf1 CKO mice the transcription of *Atf6* is downregulated, leading to a reduction in ATF6 target gene expression and a downregulation of the ERAD machinery (Fig. 5D).

Direct regulation of ERAD gene expression by Nrf1. The fact that additional ERAD factors, which have not previously been shown to be ATF6 target genes, were also downregulated in Nrf1 CKO mice prompted us to investigate whether Nrf1 may also directly regulate ERAD gene expression. Further analysis of the ChIP-Seq data revealed Nrf1 binding sites in the promoters of the genes *Ufd1l*, *Nploc4*, and *VCP* (Fig. 6A to C). The significance of this binding was confirmed by ChIP-qPCR, which revealed substantial enrichment of Nrf1 binding at the promoters of *Ufd1l*, *Nploc4*, and *VCP* compared with the negative control locus *Txs* (Fig. 6D). Interestingly, Ufd1l, Nploc4, and VCP function together to form the Cdc48 complex, which plays a pivotal role in ERAD substrate retrotranslocation from the ER, which suggests that Nrf1 activity specifically regulates this part of the ERAD pathway (7).

Nrf1 does not impact the IRE1 and PERK ER stress sensor pathways. Although RT-qPCR analysis revealed no change in *Ire1* or *Perk* expression in Nrf1 CKO mice (Fig. 1C), we wanted to determine whether these pathways exhibit altered activation in the absence of Nrf1. ER stress results in the activation of IRE1, which functions as an endoribonuclease to cleave the mRNA of *XBP1*, removing an intron from the transcript to produce an active UPR transcription factor (37). Thus, detection of the spliced form

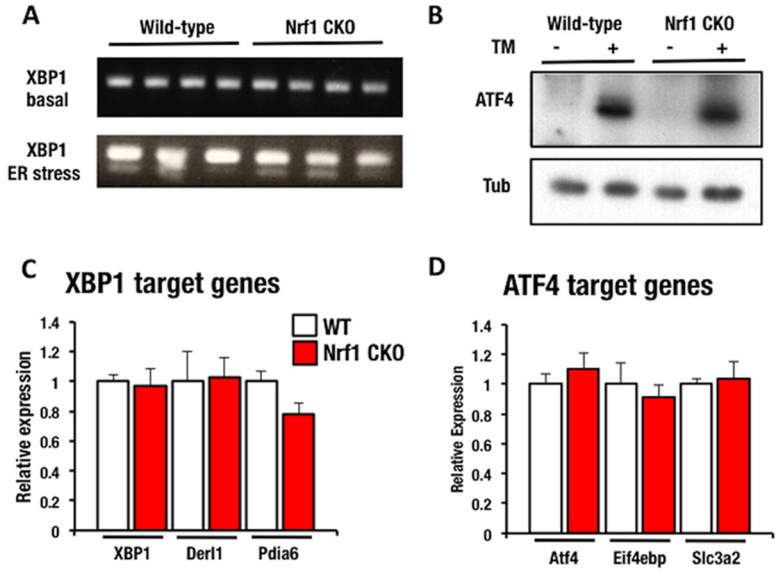

FIG 7 The IRE1 and PERK pathways are unaffected by Nrf1 deletion. (A) RT-PCR analysis of wild-type and Nrf1 CKO mice both in the basal state and treated with tunicamycin for 24 h to induce ER stress shows that the cleavage pattern of the mRNA for XBP1 is identical across genotypes. This indicates that IRE1 activity is not changed upon Nrf1 deletion. (B) Immunoblot analysis shows that at the protein level the accumulation of ATF4, under both basal and tunicamycin (TM)-induced ER stress conditions, is unaltered in Nrf1 CKO mice relative to wild-type mice. This indicates that PERK activity is not changed upon Nrf1 deletion. (C) RT-qPCR analysis shows that XBP1 target gene expression is unaltered in Nrf1 CKO mice. (D) RT-qPCR analysis shows that Atf4 target gene expression is unaltered in Nrf1 CKO mice. In both panels C and D, gene expression in Nrf1 CKO liver tissue is shown relative to the wild type, with wild-type expression fixed at 1. Error bars display the SEM ($n = 4$).

of *XBP1* mRNA can be used to assay IRE1 activity. RT-PCR analysis of the XBP1 transcript revealed no difference between the cleavage states during either basal conditions or ER stress in WT and Nrf1 CKO mice (Fig. 7A). Similarly, XBP1 target genes showed no change in expression under basal conditions in Nrf1 CKO mice, confirming that this pathway is not differentially modulated in the absence of Nrf1 (Fig. 7C).

Activation of the kinase PERK functions to enhance the activity of the transcription factor ATF4 in response to ER stress through a translation-dependent mechanism (10, 38). Thus, changes in PERK signaling activity can be assayed by measuring changes in the level of the ATF4 protein. Immunoblot analysis revealed no difference in the basal or ER stress inducible levels of ATF4, indicating that PERK activity is unchanged in Nrf1 CKO mice (Fig. 7B). As in the case of XBP1, ATF4 target genes also showed no change in expression in Nrf1 CKO mice (Fig. 7D). Taken together, these data reveal that under basal conditions, Nrf1 CKO mice are not subject to ER stress and that only the ATF6 pathway, and not the IRE1 or PERK pathways, is differentially modulated relative to wild-type mice.

***Fam134b* facilitates ER homeostasis in Nrf1 CKO mice.** A reduction in the rate of ERAD may be beneficial to cellular homeostasis in the context of Nrf1 deletion, as it will reduce the rate of flow of protein substrates to and therefore the burden on the proteasome, which exhibits reduced activity in this model. Thus, Nrf1 may function to coordinate both proteasome activity and proteasome substrate abundance. However, reduced ERAD will be accompanied by at least two potentially deleterious side effects: the physical buildup of ERAD targets in the ER, coupled with the increased risk of unfolded proteins producing deleterious effects within the cell.

Recently, the protein FAM134B has been shown to regulate ER size. Downregulation of FAM134B leads to ER expansion, a mechanism which could accommodate the increase in unfolded proteins, which may accompany reduced ERAD (39). Interestingly, preliminary data suggest that *Fam134b* expression is significantly downregulated in the unstressed Nrf1 CKO liver (see Fig. S1 in the supplemental material). Similarly, we

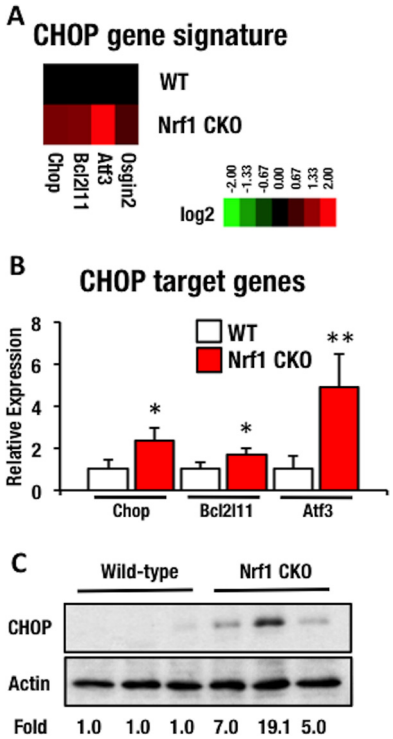

FIG 8 A CHOP-dependent gene signature in upregulated in Nrf1 CKO mice. (A) A microarray comparing gene expression in Nrf1 CKO liver and WT liver tissue revealed a significant increase in expression of *Chop*, in addition to the CHOP target genes *Bcl2l11*, *Atf3*, and *Osgin2*. (B) RT-qPCR analysis of CHOP target genes confirmed the microarray data, showing that a CHOP-dependent gene signature is significantly upregulated in Nrf1 CKO liver in comparison to wild-type tissue. (C) Immunoblot analysis of three wild-type and Nrf1 CKO mice clearly shows that at the protein level the cellular abundance of CHOP is increased in Nrf1 CKO cells. Gene expression in Nrf1 CKO liver tissue is shown relative to the wild type, with wild-type expression fixed at 1. Error bars display the SEM ($n = 4$; *, $P < 0.05$; **, $P < 0.01$).

previously observed increased polar lipid content in the liver of Nrf1 CKO mice, which would provide the lipid substrates for increased ER membrane synthesis required for ER expansion (23). Note that while in WT mice tunicamycin induced ER stress leads to a reduction in *Fam134b* expression, presumably to accommodate ER expansion, *Fam134b* expression is increased back to WT basal levels in tunicamycin-treated Nrf1 CKO liver, suggesting the existence of a homeostatic mechanism to carefully regulate ER expansion and where too much expansion is detrimental for cell survival (see Fig. S1 in the supplemental material).

CHOP-dependent gene expression is upregulated in Nrf1 CKO mice. Interestingly, in addition to revealing the downregulation of ERAD components, the Nrf1 CKO microarray also revealed an increase in expression of the transcription factor *Chop*, as well as the CHOP target genes *Bcl2l11*, *Atf3*, and *Osgin2* (Fig. 8A) (40, 41). To confirm the significance of the upregulation of *Chop* and the CHOP-dependent target genes in Nrf1 CKO mice, we carried out RT-qPCR analysis. In accordance with the microarray data, the RT-qPCR showed significant upregulation of the CHOP gene signature in Nrf1 CKO mice (Fig. 8B). To further verify that the upregulation of CHOP expression is physiologically significant, we carried out immunoblot analysis, which clearly showed that the CHOP protein is upregulated in Nrf1 CKO mouse livers (Fig. 8C). CHOP is also a transcription factor that plays a key role in the unfolded protein response, confirming the fact that Nrf1 plays an important role in the regulation of ER homeostasis (42). Canonical CHOP signaling is dependent on ATF4 activity, which is induced by ER stress in a PERK-dependent manner (10, 38). However, RT-qPCR revealed no change in Atf4 expression in Nrf1 CKO mice, and similarly, immunoblot analysis revealed no change in the level of ATF4 protein, which together suggest that in the absence of Nrf1, CHOP is regulated

in an ATF4-independent manner (Fig. 7B and D). Since CHOP regulates the expression of genes involved in apoptosis, these data suggest that the downregulation of ERAD is accompanied by the upregulation of CHOP, which functions as a compensatory mechanism, and primes cells for apoptosis in the event of further stress.

Nrf1 CKO mice are primed for an enhanced ER stress-dependent CHOP response. To test the hypothesis that increased CHOP expression in the basal state will promote an enhanced CHOP response when cells are stressed, we treated WT and Nrf1 CKO mice with tunicamycin for 24 h to induce ER stress. Although WT mice exhibited a robust 10-fold increase in *Chop* expression, Nrf1 CKO mice increased *Chop* expression by 35-fold (Fig. 9A). Similarly, expression of the CHOP target genes *Gadd34*, *Bax*, *Puma*, *Bcl2l11*, and *Atf3* was significantly enhanced in Nrf1 CKO mice, suggesting that the increase in *Chop* expression is functionally important (Fig. 9B) (43–45).

To test the generality of this homeostatic mechanism, we treated WT and Nrf1 KO MEFs with the proteasome inhibitor MG132 for 6 h, which is insufficient to cause ER stress, as an alternative stress model (46). Interestingly, in response to proteasome inhibition, we also observed an increased induction of the CHOP-dependent gene signature in Nrf1 KO cells (Fig. 9C). This suggests that upregulation of CHOP is a general homeostatic mechanism that couples the regulation of proteasome activity with CHOP-dependent apoptosis in order to mitigate the harmful effects caused by the accumulation of damaged proteins.

In order to determine whether the increased CHOP response in Nrf1 KO cells results in increased cell death, we treated WT and Nrf1 KO MEFs with MG132 or tunicamycin for 24 h in order to subject the cells to sustained stress conditions. In complete agreement with our model, Nrf1 KO cells showed significantly reduced survival in response to both MG132 and tunicamycin treatment (Fig. 9D). This supports our contention that in the absence of Nrf1 increased CHOP signaling primes cells for death in response to further stress.

DISCUSSION

Since Nrf1 plays a central role in the regulation of proteasome activity, and the proteasome facilitates efficient ER-associated degradation of ER-resident proteins, we hypothesized that Nrf1 is transcriptionally integrated into the ER homeostasis pathway. Utilizing an Nrf1 liver-specific conditional knockout mouse system, we found in this study that the ER stress sensor ATF6 and the ATF6-dependent transcription program are significantly downregulated in the absence of Nrf1. ATF6 regulates ERAD gene expression and, significantly, many ERAD components are downregulated in Nrf1 CKO mice. As summarized in Fig. 10, these results demonstrate that loss of Nrf1 leads to a homeostatic shift through which ERAD activity is reduced in order to compensate for a loss of proteasome activity.

Consistent with the hypothesis that Nrf1 regulates ER homeostasis, the single gene ablation of Nrf1, and the ER stress sensor genes *Atf6*, *Ire1*, and *Perk/eIF2*α in the mouse liver all give rise to the same phenotype, namely, the development of fatty liver, suggesting that Nrf1 and the UPR sensor proteins may regulate similar cellular processes (24, 47). Indeed, through RT-qPCR analysis, we found that *Atf6* is significantly downregulated in Nrf1 CKO mice. Furthermore, our mouse liver microarray revealed that in the basal state, genes associated with ERAD and protein processing in the ER are downregulated in Nrf1 CKO hepatocytes. Since the UPR sensor protein ATF6 regulates ERAD-associated gene expression, these data indicate that the downregulation of *Atf6* in Nrf1 CKO mice is functionally important and significantly impacts ER homeostasis. Global analysis of Nrf1 binding sites within the mouse genome revealed that Nrf1 can bind to an enhancer element within the *Atf6* locus, supporting the notion that Nrf1 regulates ERAD, at least in part, through the direct regulation of *Atf6*. We also found Nrf1 binding sites in the promoter regions of the ERAD factors *Ufd1l*, *Nploc4*, and *VCP*, which together form the Cdc48 retrotranslocase complex (7). This suggests that Nrf1 can also directly regulate the activity of ERAD components. Interestingly, it has previ-

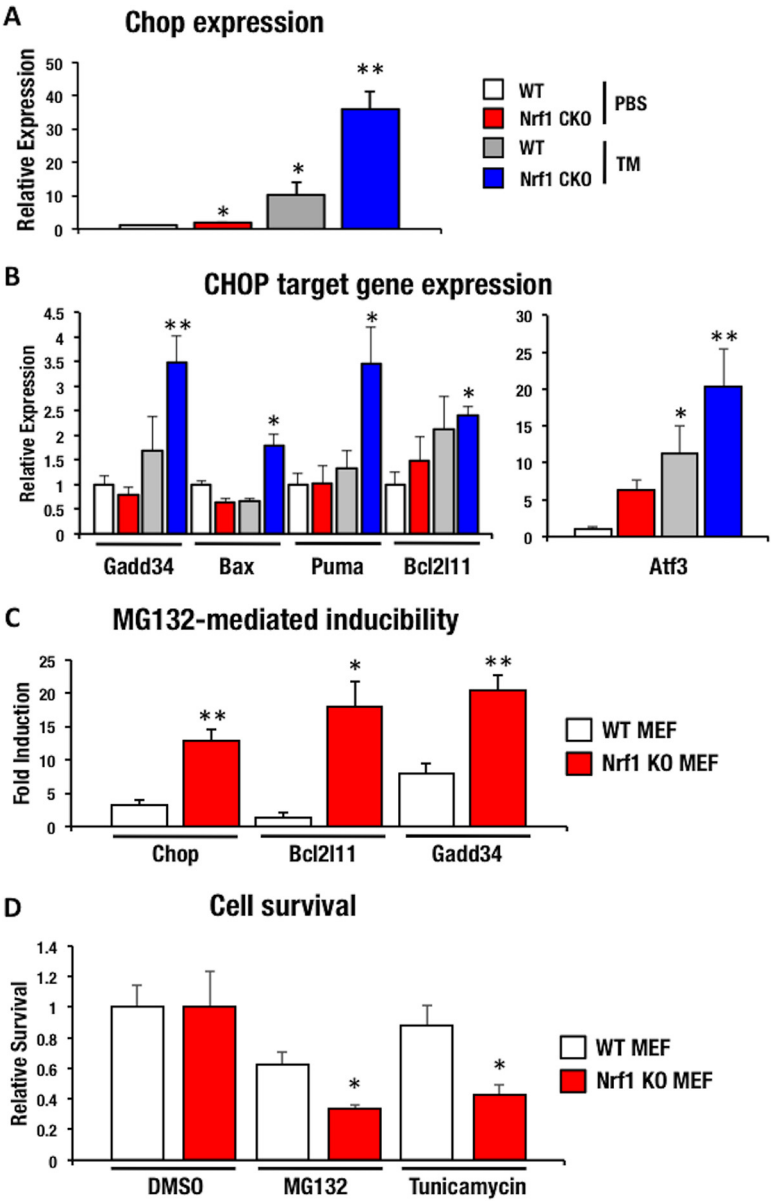

FIG 9 Cellular stress significantly increases the CHOP-dependent gene expression in Nrf1 CKO mice and Nrf1 KO fibroblasts. (A) Tunicamycin treatment leads to a significant increase in *Chop* expression in Nrf1 CKO mice. Both wild-type and Nrf1 CKO mice exhibit increased *Chop* expression in response to tunicamycin-induced ER stress; however, the increase in *Chop* expression in Nrf1 CKO mice is significantly enhanced relative to wild-type mice. (B) Tunicamycin treatment leads to a significant increase in a CHOP-dependent gene expression signature, represented by the CHOP target genes *Gadd34*, *Bax*, *Puma*, *Bcl2l11*, and *Atf3* in Nrf1 CKO mice relative to wild-type mice. (C) As an alternative stress model, MG132-mediated proteasome inhibition leads to a significant enhancement in the transcriptional induction of *Chop*, and the CHOP target genes *Bcl2l11* and *Gadd34* in Nrf1 KO fibroblasts compared to wild-type fibroblasts. The data are presented as the fold induction of gene expression, with the basal expression level set at 1. Error bars display the SEM ($n = 3$). (D) Treatment of wild-type and Nrf1 KO MEFs with the stressing agents MG132 and tunicamycin for 24 h shows a significant increase in cell death in Nrf1 KO cells relative to wild-type cells. In both panels A and B, gene expression in Nrf1 CKO liver tissue is shown relative to the wild type, with wild-type expression in response to PBS fixed at 1. Error bars display the SEM ($n = 6$; *, $P < 0.05$; **, $P < 0.01$).

ously been shown that Nrf1 activity is regulated by the ERAD machinery, indicating that an Nrf1-dependent feedback loop plays a key role in the regulation of ERAD (18, 27).

ER homeostasis is significantly impacted by ER stress (13). One consequence of ER stress is a global reduction in protein translation, which is mediated by the PERK-

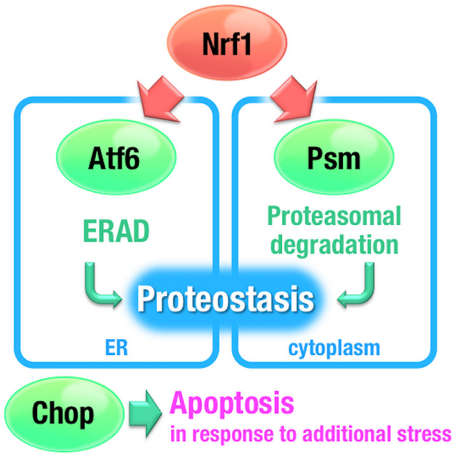

FIG 10 Nrf1-dependent regulation of ATF6 integrates the ERAD and proteasome transcriptional programs. Nrf1 regulates the transcription of the proteasome subunit genes, and therefore the loss of Nrf1 leads to a reduction in proteasome activity. Through the direct regulation of ATF6, downregulation of Nrf1 results in a decrease in ERAD, which reduces the flow of protein substrates to the proteasome, resulting in a homeostatic shift which allows cells to survive in response to decreased proteasome activity. Since the downregulation of ERAD may make cells vulnerable to the deleterious effects of unfolded proteins, reduced proteasome activity, reduced proteasome activity is coupled with increased CHOP activity, which primes cells for apoptosis in response to further stress.

dependent phosphorylation of the translation initiation factor eIF2α (10). A reduction in protein translation reduces the flow of proteins into the ER, which functions to alleviate ER stress and promote ER homeostasis (38). Interestingly, inhibition of Nrf1 activity in mouse fibroblasts has also been shown to reduce the rate of protein synthesis, in this case due to a reduction in the intracellular amino acid level (48). Thus, the cellular response to Nrf1 loss mirrors the ER stress phenotype, which supports our contention that Nrf1 is integrated into the ER homeostasis pathway.

The downregulation of ATF6 and ERAD in Nrf1 CKO mice would appear to be detrimental for cell viability, since it may make cells more susceptible to damage in response to further stress. Intriguingly, we found that the potentially deleterious effects associated with reduced ERAD are coupled with an increase in the expression of CHOP, a UPR transcription factor that can promote apoptosis (49). Since our ChIP-Seq analysis did not reveal any Nrf1 binding sites in the *Chop* locus, this increase in CHOP expression may not be directly dependent on Nrf1 transcriptional activity.

It has been shown that in fibroblasts the Nrf1-dependent reduction in proteasome activity directly results in a decrease in the cellular amino acid pool (48). Interestingly, amino acid limitation has been shown to regulate *Chop* expression through an ER-stress independent pathway (50, 51). Therefore, we surmise that one plausible explanation for the increased CHOP found in Nrf1 CKO mice is increased *Chop* expression mediated by the Nrf1-dependent reduction in proteasome activity, which reduces cellular amino acid levels. We infer that increased *Chop* expression alone is insufficient to induce cell death, since other stress induced signals, such as p38-mediated phosphorylation, are required for full CHOP activity, suggesting that Nrf1 CKO cells become "primed" for apoptosis in case of further stress (40, 52). Similarly, *Atf6* KO mice exhibit enhanced CHOP activation in response to stress, further supporting the similarities between the loss-of-Nrf1 and loss-of-ATF6 phenotypes (34, 35). Since we did not observe an increase in ATF4 signaling in Nrf1 CKO mice, the increased *Chop* expression may be due to noncanonical regulation, such as through pathways dependent on AP1 or retinoic acid signaling (53, 54).

Significantly, loss of Nrf1 has been shown to result in an increase in autophagy, a homeostatic shift that would allow cells to degrade damaged proteins through an alternate pathway in response to reduced ERAD and proteasome activity (55). Together, these data strongly argue that Nrf1 is an integral member of the proteostasis network,

which can regulate both cytoplasmic and ER proteostasis, and trigger apoptosis if the balance between damage and repair becomes unfavorable for cell viability.

Showing very good agreement with this idea, Nrf1-deficient cells are susceptible to cell death in response to a variety of stresses. For example, we found that Nrf1 KO cells exhibit increased susceptibility to cell death in response to sustained proteasome inhibition or ER stress, whereas during embryogenesis, Nrf1 knockout hepatocytes die due to ROS induced apoptosis. Similarly, *in vitro*, Nrf1-deficient cells show increased sensitivity to tumor necrosis factor alpha, tBHP, UVB, and inorganic arsenic-induced apoptosis (56–58). Interestingly, overexpression of Nrf1 has been shown to protect cells from apoptosis. Thus, in the chick limb bud, the overexpression of Nrf1, but not that of Nrf2 or XBP1, was shown to lead to a reduction in apoptosis during limb morphogenesis (59).

A reduction in ERAD in Nrf1 CKO mice may lead to the physical accumulation of ERAD substrates in the ER, which could have deleterious consequences for the cell. Recently, the protein FAM134B has been shown to regulate the size of the ER by facilitating ER degradation by autophagy (39). Loss of the *Fam134b* gene expression was shown to lead to ER expansion and a sensitization of cells to further stress. Interestingly, we also observed a reduction in *Fam134b* mRNA expression in Nrf1 CKO mice, suggesting that this may facilitate ER expansion to cope with a reduction in ERAD. As in the case of CHOP, changes in FAM134B level in Nrf1 CKO cells may make cells more sensitive to further stress. Thus, increased *Chop* expression, coupled with decreased *Fam134b* expression, acts as a safety valve, which allows cells to survive under homeostatic conditions but can promote apoptosis during periods of cell stress. Therefore, our data show that Nrf1 is intimately integrated into the ER homeostasis pathway and that alterations in Nrf1 activity lead to a wide range of gene expression changes which function to maintain cellular homeostasis.

To our knowledge, this study represents the first ChIP-Seq experiment for Nrf1. Analysis of these data allowed us to determine the Nrf1 binding site to be (A/G)TGA CTCAGC. Of note, this binding site is identical to the site identified for the related factor Nrf2 (28). Although it is common for related factors to have similar consensus binding sites, it is of interest that the target genes for Nrf1 and Nrf2 show very little overlap, as shown in Fig. 2H. This finding supports previous reports in which the activities of Nrf1 and Nrf2 in the mouse liver were found to be distinct (20, 22). Thus, while Nrf1 regulates expression of proteasome subunits and ER homeostasis, Nrf2 regulates genes involved in the cellular response to oxidative stress and the maintenance of redox homeostasis (20). These data indicate that variables other than the consensus binding sequence of Nrf1 and Nrf2 determine the genes that they regulate. One plausible explanation for this difference is that Nrf2 regulates transcription in part by recruiting other transcription factors to enhancer elements, including the recruitment of (i) the chromatin remodeling factor BRG1 to the *HO-1* locus, (ii) ATF4 for the regulation of *xCT* expression, and (iii) the mediator component Med16 for the modulation of multiple target genes (60–62). Thus, the presence or absence of cofactors may play a large role in determining Nrf1 and Nrf2-dependent target gene expression.

Interestingly, the *Caenorhabditis elegans* homologue of Nrf1 and Nrf2, SKN-1, combines the activities of Nrf1 and Nrf2 into a single factor and as such regulates proteasome gene expression, ER homeostasis, antioxidant gene expression, and redox balance (63, 64). Thus, it appears that the SKN-1/Nrf family of proteins represent an excellent example of protein subfunctionalization, in which the ancestral functions of SKN-1 have been partitioned into two mammalian factors, Nrf1 and Nrf2, to allow finer regulatory control over critical homeostatic processes (65).

In summary, we found that Nrf1 regulates the transcription of the ER stress sensor gene *Atf6*. This directly leads to an ATF6-dependent downregulation of the ERAD transcriptional program in Nrf1-deficient cells. As in the absence of Nrf1, proteasome gene expression, and thus proteasome activity, is reduced, the concomitant reduction in ERAD allows cells to maintain homeostasis by limiting the flow of substrates through the degradation machinery, which reduces the burden on the proteasome. Since

alterations in protein homeostasis play a central role in many human pathologies, including neurodegenerative diseases and cancer, this study provides fresh insight into the transcriptional integration of proteostasis regulation.

MATERIALS AND METHODS

Nrf1 CKO mouse lines. Nrf1 floxed mice (*Nrf1*$^{flox/flox}$) and liver-specific inducible Nrf1 knockout mice (*Nrf1*$^{flox/flox}$::*CYP1A1-Cre*) were generated as described previously (23). In this study, 3-methylcholanthrene (3-MC) was dissolved in corn oil at a dose of 4.0 mg/ml and was administered to *Nrf1*$^{flox/flox}$ or *Nrf1*$^{flox/flox}$::*CYP1A1-Cre* male mice as a single subcutaneous injection to give a dose of 40 mg/kg (body weight). At 2 weeks after the 3-MC injection, the mice were sacrificed, with livers from *Nrf1*$^{flox/flox}$::*CYP1A1-Cre* mice treated with 3-MC used for the Nrf1 CKO group and livers from *Nrf1*$^{flox/flox}$ treated with 3-MC used as wild-type controls. Tunicamycin injections (1 mg/kg [body weight]) were carried out as previously described (34). The mice were sacrificed 24 h after the tunicamycin injection, after which the livers were removed for analysis. Tunicamycin was purchased from Tocris Bioscience (Bristol, United Kingdom).

Cell culture. Mouse embryonic fibroblasts (MEFs) were immortalized with SV40 large T antigen. MEF cells were maintained in Dulbecco modified Eagle medium supplemented with 10% fetal bovine serum and antibiotics. Where indicated, cells were treated with 10 μM MG132 for 6 h. MG132 was purchased from Peptide Institute, Inc. (Osaka, Japan).

ChIP. ChIP was performed on SV40 large T antigen immortalized wild-type MEFs, using an anti-TCF11 antibody, as described previously (66). Briefly, approximately 7 $\times$ 10^6 fibroblasts were fixed with 1% formaldehyde for 10 min at room temperature. The fixed cells were neutralized with 1.25 M glycine and washed three times with ice-cold phosphate-buffered saline (PBS), before being lysed in cell lysis buffer {5 mM PIPES [piperazine-*N*,*N*′-bis(2-ethanesulfonic acid]-KCl (pH 8.0), 85 mM KCl, 0.5% NP-40, 1 mM phenylmethylsulfonyl fluoride (PMSF), 1$\times$ Complete protease inhibitor cocktail (Roche, Basel, Switzerland)} for 10 min on ice. The chromatin was pelleted by centrifugation at 1,000 $\times$ *g* for 10 min at 4°C, followed by resuspension in nuclear lysis buffer (50 mM Tris-HCl [pH 8.0], 10 mM EDTA, 1% sodium dodecyl sulfate, 1 mM PMSF, 1$\times$ Complete protease inhibitor cocktail [Roche]) and sonication on ice. The chromatin was incubated with the anti-TCF11 antibody and immunoabsorbed with a mixture of protein A and protein G Dynabeads (Life Technologies, Carlsbad, CA).

ChIP sequencing (ChIP-Seq) and analysis. Approximately 1 ng of each ChIP and input samples were used to prepare ChIP-Seq libraries using the Ovation Ultralow DR Multiplex System 1-8 (NuGEN, 0330-32). Libraries clonally amplified in a flow cell were sequenced with Illumina Hiseq 2500 (Illumina). Paired-end-sequenced reads were mapped to the mouse genome (67) (mm9) with bwa (68) (v0.6.2-r126). Paired reads uniquely mapped to the genome were extracted using samtools (69) (v0.1.18). Peak call was executed with a model-based analysis of ChIP-Seq (70) (macs, v2.0.10), and peaks were annotated with BEDtools (71) (v2.17.0).

Antibodies. Anti-TCF11 (D5B10) antibody 8052, anti-CHOP (L63F7) antibody 2895, and anti-ATF4 (D4B8) antibody 11815 were purchased from Cell Signaling Technology. Anti-ATF6 antibody (ab203119) was purchased from Abcam, antiactin (C-11) SC-1615 was purchased from Santa Cruz Biotechnology, and antitubulin (T9026) was purchased from Sigma-Aldrich.

Gene expression analysis by qPCR. Total RNA was prepared from snap-frozen liver samples using TRIzol reagent (Life Technologies) in accordance with the manufacturer's instructions. A 1-μg aliquot of total RNA was reverse transcribed with ReverTra Ace (Toyobo, Osaka, Japan). The resultant cDNA was used as a temperate for quantitative reverse transcription-PCR (RT-qPCR) on a SYBR green 7300 real-time PCR analyzer (Life Technologies). The primers used during the qPCR analysis are listed in Tables S1 and S2 in the supplemental material.

Microarray analysis and data mining. Microarray analysis were conducted with four independent RNA samples from Nrf1 conditional knockout and control groups using Agilent 8$\times$60K whole-mouse genome oligonucleotide microarray slides. Briefly, purified RNA was hybridized onto microarray slides, washed and scanned on an Agilent microarray scanner according to the Agilent protocol. The scanned fluorescent data were converted to expression data and subjected to statistical analysis using GeneSpring software (Agilent).

Cell survival assay. A total of 4.0 $\times$ 10^4 wild-type and Nrf1 KO MEFs were plated into individual wells of a 96-well plate. The cells were treated with either dimethyl sulfoxide, 1 μM MG132, or tunicamycin at 2 μg/ml for 24 h. Cell survival was measured using the CellTiter 96 MTT reagent according to the manufacturer's instructions (Promega) and quantified using a PHERAstar FS microplate reader (BMG Labtech, Ortenberg, Germany).

Statistical analysis. All data are presented as means $\pm$ the standard errors of the means (SEM). Statistical analysis was performed using a two-tail Student *t* test. Immunoblot quantification was carried out using ImageJ (National Institutes of Health, Bethesda, MD).

Accession number(s). The Nrf1 ChIP-Seq data are available from GEO (Gene Expression Omnibus) under accession number GSE89344. The wild-type and Nrf1 CKO liver microarray data are also available from GEO under accession number GSE89310.

SUPPLEMENTAL MATERIAL

Supplemental material for this article may be found at https://doi.org/10.1128/MCB.00439-16.

TEXT S1, PDF file, 0.2 MB.
TEXT S2, PDF file, 0.3 MB.
TEXT S3, PDF file, 0.8 MB.

ACKNOWLEDGMENTS

We thank M. Tsuda, M. Kikuchi, M. Nakagawa, and K. Kuroda for technical assistance and S. Goto for assistance with the mouse work. We also acknowledge the technical support of the Biomedical Research Core of Tohoku University Graduate School of Medicine and all members of the Department of Medical Biochemistry laboratory for valuable discussions.

This study was supported in part by Platform for Drug Discovery, Informatics, and Structural Life Science from the MEXT, Japan (T.T. and M.Y.), JSPS KAKENHI grant 25750357 (T.T.), and the Adaptable and Seamless Technology Transfer Program through target-driven R&D (A-STEP), Japan Science and Technology Agency grant J120001909 (T.T.).

REFERENCES

1. Powers ET, Balch WE. 2013. Diversity in the origins of proteostasis networks: a driver for protein function in evolution. Nat Rev Mol Cell Biol 14:237–248. https://doi.org/10.1038/nrm3542.
2. Kaushik S, Cuervo AM. 2015. Proteostasis and aging. Nat Med 21:1406–1415. https://doi.org/10.1038/nm.4001.
3. López-Otín C, Blasco MA, Partridge L, Serrano M, Kroemer G. 2013. The hallmarks of aging. Cell 153:1194–1217. https://doi.org/10.1016/j.cell.2013.05.039.
4. Vilchez D, Saez I, Dillin A. 2014. The role of protein clearance mechanisms in organismal ageing and age-related diseases. Nat Commun 5:5659. https://doi.org/10.1038/ncomms6659.
5. Wang M, Kaufman RJ. 2016. Protein misfolding in the endoplasmic reticulum as a conduit to human disease. Nature 529:326–335. https://doi.org/10.1038/nature17041.
6. Christianson JC, Olzmann JA, Shaler TA, Sowa ME, Bennett EJ, Richter CM, Tyler RE, Greenblatt EJ, Harper JW, Kopito RR. 2011. Defining human ERAD networks through an integrative mapping strategy. Nat Cell Biol 14:93–105. https://doi.org/10.1038/ncb2383.
7. Vembar SS, Brodsky JL. 2008. One step at a time: endoplasmic reticulum-associated degradation. Nat Rev Mol Cell Biol 9:944–957. https://doi.org/10.1038/nrm2546.
8. Hetz C. 2012. The unfolded protein response: controlling cell fate decisions under ER stress and beyond. Nat Rev Mol Cell Biol 13:89–102. https://doi.org/10.1038/nrm3270.
9. Cox JS, Shamu CE, Walter P. 1993. Transcriptional induction of genes encoding endoplasmic reticulum resident proteins requires a transmembrane protein kinase. Cell 73:1197–1206. https://doi.org/10.1016/0092-8674(93)90648-A.
10. Harding HP, Zhang Y, Ron D. 1999. Protein translation and folding are coupled by an endoplasmic-reticulum-resident kinase. Nature 397:271–274. https://doi.org/10.1038/16729.
11. Haze K, Yoshida H, Yanagi H, Yura T, Mori K. 1999. Mammalian transcription factor ATF6 is synthesized as a transmembrane protein and activated by proteolysis in response to endoplasmic reticulum stress. Mol Biol Cell 10:3787–3799. https://doi.org/10.1091/mbc.10.11.3787.
12. Mori K, Ma W, Gething MJ, Sambrook J. 1993. A transmembrane protein with a cdc2^{+}/CDC28-related kinase activity is required for signaling from the ER to the nucleus. Cell 74:743–756. https://doi.org/10.1016/0092-8674(93)90521-Q.
13. Ron D, Walter P. 2007. Signal integration in the endoplasmic reticulum unfolded protein response. Nat Rev Mol Cell Biol 8:519–529. https://doi.org/10.1038/nrm2199.
14. Hiller MM, Finger A, Schweiger M, Wolf DH. 1996. ER degradation of a misfolded luminal protein by the cytosolic ubiquitin-proteasome pathway. Science 273:1725–1728. https://doi.org/10.1126/science.273.5282.1725.
15. Werner ED, Brodsky JL, McCracken AA. 1996. Proteasome-dependent endoplasmic reticulum-associated protein degradation: an unconventional route to a familiar fate. Proc Natl Acad Sci U S A 93:13797–13801. https://doi.org/10.1073/pnas.93.24.13797.
16. Wiertz EJ, Tortorella D, Bogyo M, Yu J, Mothes W, Jones TR, Rapoport TA, Ploegh HL. 1996. Sec61-mediated transfer of a membrane protein from the endoplasmic reticulum to the proteasome for destruction. Nature 384:432–438. https://doi.org/10.1038/384432a0.
17. Radhakrishnan SK, Lee CS, Young P, Beskow A, Chan JY, Deshaies RJ. 2010. Transcription factor Nrf1 mediates the proteasome recovery pathway after proteasome inhibition in mammalian cells. Mol Cell 38:17–28. https://doi.org/10.1016/j.molcel.2010.02.029.
18. Steffen J, Seeger M, Koch A, Krüger E. 2010. Proteasomal degradation is transcriptionally controlled by TCF11 via an ERAD-dependent feedback loop. Mol Cell 40:147–158. https://doi.org/10.1016/j.molcel.2010.09.012.
19. Chan JY, Kwong M, Lu R, Chang J, Wang B, Yen TS, Kan YW. 1998. Targeted disruption of the ubiquitous CNC-bZIP transcription factor, Nrf-1, results in anemia and embryonic lethality in mice. EMBO J 17:1779–1787. https://doi.org/10.1093/emboj/17.6.1779.
20. Hirotsu Y, Hataya N, Katsuoka F, Yamamoto M. 2012. NF-E2-related factor 1 (Nrf1) serves as a novel regulator of hepatic lipid metabolism through regulation of the Lipin1 and PGC-1β genes. Mol Cell Biol 32:2760–2770. https://doi.org/10.1128/MCB.06706-11.
21. Lee CS, Lee C, Hu T, Nguyen JM, Zhang J, Martin MV, Vawter MP, Huang EJ, Chan JY. 2011. Loss of nuclear factor E2-related factor 1 in the brain leads to dysregulation of proteasome gene expression and neurodegeneration. Proc Natl Acad Sci U S A 108:8408–8413. https://doi.org/10.1073/pnas.1019209108.
22. Ohtsuji M, Katsuoka F, Kobayashi A, Aburatani H, Hayes JD, Yamamoto M. 2008. Nrf1 and Nrf2 play distinct roles in activation of antioxidant response element-dependent genes. J Biol Chem 283:33554–33562. https://doi.org/10.1074/jbc.M804597200.
23. Tsujita T, Peirce V, Baird L, Matsuyama Y, Takaku M, Walsh SV, Griffin JL, Uruno A, Yamamoto M, Hayes JD. 2014. Transcription factor Nrf1 negatively regulates the cystine/glutamate transporter and lipid-metabolizing enzymes. Mol Cell Biol 34:3800–3816. https://doi.org/10.1128/MCB.00110-14.
24. Xu Z, Chen L, Leung L, Yen TS, Lee C, Chan JY. 2005. Liver-specific inactivation of the Nrf1 gene in adult mouse leads to nonalcoholic steatohepatitis and hepatic neoplasia. Proc Natl Acad Sci U S A 102:4120–4125. https://doi.org/10.1073/pnas.0500660102.
25. Wang W, Chan JY. 2006. Nrf1 is targeted to the endoplasmic reticulum membrane by an N-terminal transmembrane domain: inhibition of nuclear translocation and transacting function. J Biol Chem 281:19676–19687. https://doi.org/10.1074/jbc.M602802200.
26. Zhang Y, Crouch DH, Yamamoto M, Hayes JD. 2006. Negative regulation of the Nrf1 transcription factor by its N-terminal domain is independent of Keap1: Nrf1, but not Nrf2, is targeted to the endoplasmic reticulum. Biochem J 399:373–385. https://doi.org/10.1042/BJ20060725.
27. Radhakrishnan SK, den Besten W, Deshaies RJ. 2014. p97-dependent retrotranslocation and proteolytic processing govern formation of active Nrf1 upon proteasome inhibition. eLife 3:e01856.
28. Hirotsu Y, Katsuoka F, Funayama R, Nagashima T, Nishida Y, Nakayama K, Engel JD, Yamamoto M. 2012. Nrf2-MafG heterodimers contribute

globally to antioxidant and metabolic networks. Nucleic Acids Res 40: 10228–10239. https://doi.org/10.1093/nar/gks827.
29. Machanick P, Bailey TL. 2011. MEME-ChIP: motif analysis of large DNA datasets. Bioinformatics 27:1696–1697. https://doi.org/10.1093/bioinformatics/btr189.
30. Johnsen O, Skammelsrud N, Luna L, Nishizawa M, Prydz H, Kolstø AB. 1996. Small Maf proteins interact with the human transcription factor TCF11/Nrf1/LCR-F1. Nucleic Acids Res 24:4289–4297. https://doi.org/10.1093/nar/24.21.4289.
31. Rosenbloom KR, Armstrong J, Barber GP, Casper J, Clawson H, Diekhans M, Dreszer TR, Fujita PA, Guruvadoo L, Haeussler M, Harte RA, Heitner S, Hickey G, Hinrichs AS, Hubley R, Karolchik D, Learned K, Lee BT, Li CH, Miga KH, Nguyen N, Paten B, Raney BJ, Smit AF, Speir ML, Zweig AS, Haussler D, Kuhn RM, Kent WJ. 2015. The UCSC Genome Browser database: 2015 update. Nucleic Acids Res 43:D670–D681. https://doi.org/10.1093/nar/gku1177.
32. Zhang J, Hosoya T, Maruyama A, Nishikawa K, Maher JM, Ohta T, Motohashi H, Fukamizu A, Shibahara S, Itoh K, Yamamoto M. 2007. Nrf2 Neh5 domain is differentially utilized in the transactivation of cytoprotective genes. Biochem J 404:459–466. https://doi.org/10.1042/BJ20061611.
33. Shlyueva D, Stampfel G, Stark A. 2014. Transcriptional enhancers: from properties to genome-wide predictions. Nat Rev Genet 15:272–286. https://doi.org/10.1038/nrg3682.
34. Wu J, Rutkowski DT, Dubois M, Swathirajan J, Saunders T, Wang J, Song B, Yau GD, Kaufman RJ. 2007. ATF6alpha optimizes long-term endoplasmic reticulum function to protect cells from chronic stress. Dev Cell 13:351–364. https://doi.org/10.1016/j.devcel.2007.07.005.
35. Yamamoto K, Sato T, Matsui T, Sato M, Okada T, Yoshida H, Harada A, Mori K. 2007. Transcriptional induction of mammalian ER quality control proteins is mediated by single or combined action of ATF6α and XBP1. Dev Cell 13:365–376. https://doi.org/10.1016/j.devcel.2007.07.018.
36. Shoulders MD, Ryno LM, Genereux JC, Moresco JJ, Tu PG, Wu C, Yates JR, III, Su AI, Kelly JW, Wiseman RL. 2013. Stress-independent activation of XBP1s and/or ATF6 reveals three functionally diverse ER proteostasis environments. Cell Rep 3:1279–1292. https://doi.org/10.1016/j.celrep.2013.03.024.
37. Calfon M, Zeng H, Urano F, Till JH, Hubbard SR, Harding HP, Clark SG, Ron D. 2002. IRE1 couples endoplasmic reticulum load to secretory capacity by processing the XBP-1 mRNA. Nature 415:92–96. https://doi.org/10.1038/415092a.
38. Harding HP, Novoa I, Zhang Y, Zeng H, Wek R, Schapira M, Ron D. 2000. Regulated translation initiation controls stress-induced gene expression in mammalian cells. Mol Cell 6:1099–1108. https://doi.org/10.1016/S1097-2765(00)00108-8.
39. Khaminets A, Heinrich T, Mari M, Grumati P, Huebner AK, Akutsu M, Liebmann L, Stolz A, Nietzsche S, Koch N, Mauthe M, Katona I, Qualmann B, Weis J, Reggiori F, Kurth I, Hübner CA, Dikic I. 2015. Regulation of endoplasmic reticulum turnover by selective autophagy. Nature 522: 354–358. https://doi.org/10.1038/nature14498.
40. Han J, Back SH, Hur J, Lin YH, Gildersleeve R, Shan J, Yuan CL, Krokowski D, Wang S, Hatzoglou M, Kilberg MS, Sartor MA, Kaufman RJ. 2013. ER-stress-induced transcriptional regulation increases protein synthesis leading to cell death. Nat Cell Biol 15:481–490. https://doi.org/10.1038/ncb2738.
41. Puthalakath H, O'Reilly LA, Gunn P, Lee L, Kelly PN, Huntington ND, Hughes PD, Michalak EM, McKimm-Breschkin J, Motoyama N, Gotoh T, Akira S, Bouillet P, Strasser A. 2007. ER stress triggers apoptosis by activating BH3-only protein Bim. Cell 129:1337–1349. https://doi.org/10.1016/j.cell.2007.04.027.
42. Tabas I, Ron D. 2011. Integrating the mechanisms of apoptosis induced by endoplasmic reticulum stress. Nat Cell Biol 13:184–190. https://doi.org/10.1038/ncb0311-184.
43. Cazanave SC, Elmi NA, Akazawa Y, Bronk SF, Mott JL, Gores GJ. 2010. CHOP and AP-1 cooperatively mediate PUMA expression during lipoapoptosis. Am J Physiol Gastrointest Liver Physiol 299:G236–G243. https://doi.org/10.1152/ajpgi.00091.2010.
44. Fu HY, Okada K, Liao Y, Tsukamoto O, Isomura T, Asai M, Sawada T, Okuda K, Asano Y, Sanada S, Asanuma H, Asakura M, Takashima S, Komuro I, Kitakaze M, Minamino T. 2010. Ablation of C/EBP homologous protein attenuates endoplasmic reticulum-mediated apoptosis and cardiac dysfunction induced by pressure overload. Circulation 122:361–369. https://doi.org/10.1161/CIRCULATIONAHA.109.917914.
45. Marciniak SJ, Yun CY, Oyadomari S, Novoa I, Zhang Y, Jungreis R, Nagata K, Harding HP, Ron D. 2004. CHOP induces death by promoting protein synthesis and oxidation in the stressed endoplasmic reticulum. Genes Dev 18:3066–3077. https://doi.org/10.1101/gad.1250704.
46. Teske BF, Wek SA, Bunpo P, Cundiff JK, McClintick JN, Anthony TG, Wek RC. 2011. The eIF2 kinase PERK and the integrated stress response facilitate activation of ATF6 during endoplasmic reticulum stress. Mol Biol Cell 22:4390–4405. https://doi.org/10.1091/mbc.E11-06-0510.
47. Rutkowski DT, Wu J, Back SH, Callaghan MU, Ferris SP, Iqbal J, Clark R, Miao H, Hassler JR, Fornek J, Katze MG, Hussain MM, Song B, Swathirajan J, Wang J, Yau GD, Kaufman RJ. 2008. UPR pathways combine to prevent hepatic steatosis caused by ER stress-mediated suppression of transcriptional master regulators. Dev Cell 15:829–840. https://doi.org/10.1016/j.devcel.2008.10.015.
48. Zhang Y, Nicholatos J, Dreier JR, Ricoult SJ, Widenmaier SB, Hotamisligil GS, Kwiatkowski DJ, Manning BD. 2014. Coordinated regulation of protein synthesis and degradation by mTORC1. Nature 513:440–443. https://doi.org/10.1038/nature13492.
49. Zinszner H, Kuroda M, Wang X, Batchvarova N, Lightfoot RT, Remotti H, Stevens JL, Ron D. 1998. CHOP is implicated in programmed cell death in response to impaired function of the endoplasmic reticulum. Genes Dev 12:982–995. https://doi.org/10.1101/gad.12.7.982.
50. Bruhat A, Jousse C, Wang XZ, Ron D, Ferrara M, Fafournoux P. 1997. Amino acid limitation induces expression of CHOP, a CCAAT/enhancer binding protein-related gene, at both transcriptional and posttranscriptional levels. J Biol Chem 272:17588–17593. https://doi.org/10.1074/jbc.272.28.17588.
51. Jousse C, Bruhat A, Harding HP, Ferrara M, Ron D, Fafournoux P. 1999. Amino acid limitation regulates CHOP expression through a specific pathway independent of the unfolded protein response. FEBS Lett 448:211–216. https://doi.org/10.1016/S0014-5793(99)00373-7.
52. Wang XZ, Ron D. 1996. Stress-induced phosphorylation and activation of the transcription factor CHOP (GADD153) by p38 MAP kinase. Science 272:1347–1349. https://doi.org/10.1126/science.272.5266.1347.
53. Gery S, Park DJ, Vuong PT, Chih DY, Lemp N, Koeffler HP. 2004. Retinoic acid regulates C/EBP homologous protein expression (CHOP), which negatively regulates myeloid target genes. Blood 104:3911–3917. https://doi.org/10.1182/blood-2003-10-3688.
54. Pirot P, Ortis F, Cnop M, Ma Y, Hendershot LM, Eizirik DL, Cardozo AK. 2007. Transcriptional regulation of the endoplasmic reticulum stress gene chop in pancreatic insulin-producing cells. Diabetes 56:1069. https://doi.org/10.2337/db06-1253.
55. Tsuchiya Y, Taniguchi H, Ito Y, Morita T, Karim MR, Ohtake N, Fukagai K, Ito T, Okamuro S, Iemura S, Natsume T, Nishida E, Kobayashi A. 2013. The casein kinase 2-nrf1 axis controls the clearance of ubiquitinated proteins by regulating proteasome gene expression. Mol Cell Biol 33:3461–3472. https://doi.org/10.1128/MCB.01271-12.
56. Chen L, Kwong M, Lu R, Ginzinger D, Lee C, Leung L, Chan JY. 2003. Nrf1 is critical for redox balance and survival of liver cells during development. Mol Cell Biol 23:4673–4686. https://doi.org/10.1128/MCB.23.13.4673-4686.2003.
57. Han W, Ming M, Zhao R, Pi J, Wu C, He YY. 2012. Nrf1 CNC-bZIP protein promotes cell survival and nucleotide excision repair through maintaining glutathione homeostasis. J Biol Chem 287:18788–18795. https://doi.org/10.1074/jbc.M112.363614.
58. Zhao R, Hou Y, Xue P, Woods CG, Fu J, Feng B, Guan D, Sun G, Chan JY, Waalkes MP, Andersen ME, Pi J. 2011. Long isoforms of NRF1 contribute to arsenic-induced antioxidant response in human keratinocytes. Environ Health Perspect 119:56–62. https://doi.org/10.1289/ehp.1002304.
59. Suda N, Itoh T, Nakato R, Shirakawa D, Bando M, Katou Y, Kataoka K, Shirahige K, Tickle C, Tanaka M. 2014. Dimeric combinations of MafB, cFos and cJun control the apoptosis-survival balance in limb morphogenesis. Development 141:2885–2894. https://doi.org/10.1242/dev.099150.
60. Sekine H, Okazaki K, Ota N, Shima H, Katoh Y, Suzuki N, Igarashi K, Ito M, Motohashi H, Yamamoto M. 2015. The mediator subunit MED16 transduces NRF2-activating signals into antioxidant gene expression. Mol Cell Biol 36:407–420. https://doi.org/10.1128/MCB.00785-15.
61. Ye P, Mimura J, Okada T, Sato H, Liu T, Maruyama A, Ohyama C, Itoh K. 2014. Nrf2- and ATF4-dependent upregulation of xCT modulates the sensitivity of T24 bladder carcinoma cells to proteasome inhibition. Mol Cell Biol 34:3421–3434. https://doi.org/10.1128/MCB.00221-14.
62. Zhang J, Ohta T, Maruyama A, Hosoya T, Nishikawa K, Maher JM, Shibahara S, Itoh K, Yamamoto M. 2006. BRG1 interacts with Nrf2 to

selectively mediate HO-1 induction in response to oxidative stress. Mol Cell Biol 26:7942–7952. https://doi.org/10.1128/MCB.00700-06.
63. Glover-Cutter KM, Lin S, Blackwell TK. 2013. Integration of the unfolded protein and oxidative stress responses through SKN-1/Nrf. PLoS Genet 9:e1003701. https://doi.org/10.1371/journal.pgen.1003701.
64. Oliveira RP, Porter Abate J, Dilks K, Landis J, Ashraf J, Murphy CT, Blackwell TK. 2009. Condition-adapted stress and longevity gene regulation by *Caenorhabditis elegans* SKN-1/Nrf. Aging Cell 8:524–541. https://doi.org/10.1111/j.1474-9726.2009.00501.x.
65. Innan H, Kondrashov F. 2010. The evolution of gene duplications: classifying and distinguishing between models. Nat Rev Genet 11:97–108. https://doi.org/10.1038/ni0110-97b.
66. Fujita R, Takayama-Tsujimoto M, Satoh H, Gutiérrez L, Aburatani H, Fujii S, Sarai A, Bresnick EH, Yamamoto M, Motohashi H. 2013. NF-E2 p45 is important for establishing normal function of platelets. Mol Cell Biol 33:2659–2670. https://doi.org/10.1128/MCB.01274-12.
67. Fujita PA, Rhead B, Zweig AS, Hinrichs AS, Karolchik D, Cline MS, Goldman M, Barber GP, Clawson H, Coelho A, Diekhans M, Dreszer TR, Giardine BM, Harte RA, Hillman-Jackson J, Hsu F, Kirkup V, Kuhn RM, Learned K, Li CH, Meyer LR, Pohl A, Raney BJ, Rosenbloom KR, Smith KE, Haussler D, Kent WJ. 2010. The UCSC Genome Browser database: update 2011. Nucleic Acids Res 39:D876–D882. https://doi.org/10.1093/nar/gkt1168.
68. Li H, Durbin R. 2009. Fast and accurate short read alignment with Burrows-Wheeler transform. Bioinformatics 25:1754–1760. https://doi.org/10.1093/bioinformatics/btp324.
69. Li H, Handsaker B, Wysoker A, Fennell T, Ruan J, Homer N, Marth G, Abecasis G, Durbin R; 1000 Genome Project Data Processing Subgroup. 2009. The Sequence Alignment/Map format and SAMtools. Bioinformatics 25:2078–2079. https://doi.org/10.1093/bioinformatics/btp352.
70. Zhang Y, Liu T, Meyer CA, Eeckhoute J, Johnson DS, Bernstein BE, Nusbaum C, Myers RM, Brown M, Li W, Liu XS. 2008. Model-based analysis of ChIP-Seq (MACS). Genome Biol 9:R137. https://doi.org/10.1186/gb-2008-9-9-r137.
71. Quinlan AR, Hall IM. 2010. BEDTools: a flexible suite of utilities for comparing genomic features. Bioinformatics 26:841–842. https://doi.org/10.1093/bioinformatics/btq033.